arXiv:cond-mat/0207147v1 [cond-mat.supr-con] 5 Jul 2002

Large anisotropy in the optical conductivity of YNi_2B_2C

S. J. Youn[1], B. I. Min[2], and A. J. Freeman[3]
[1] *National Creative Research Initiative Center for Superfunctional Materials and Department of Chemistry, Pohang University of Science and Technology, Pohang 790-784, Korea.*
[2] *Department of Physics, Pohang University of Science and Technology, Pohang 790-784, Korea.*
[3] *Department of Physics and Astronomy Northwestern University, Evanston, IL 60208-3112, USA*

The optical properties of YNi_2B_2C are studied by using the first-principles full-potential linearized augmented plane wave (FLAPW) method within the local density approximation. Anisotropic behavior is obtained in the optical conductivity, even though the electronic structure shows 3D character. A large peak in σ_z is obtained at 2.4 eV. The anisotropic optical properties are analyzed in terms of interband transitions between energy levels and found that the Ni site plays an important role. The electronic energy loss spectroscopy (EELS) spectra are also calculated to help elucidate the anisotropic properties in this system.

74.25.Gz, 74.25.Jb

Quaternary transition metal borocarbide superconductors with formula RM_2B_2C (R= Y, rare-earths; M=transition metal) have attracted much attention due to their relatively high superconducting transition temperatures in the intermetallic compounds including exchange enhanced transition metal elements such as Ni, Pd, and Ru [1,2]. Of special interest is the coexistence and interplay between superconductivity and magnetism in the systems containing rare-earth elements [3]. YNi_2B_2C with T_c=15.6 K serves as a reference system for understanding the superconducting mechanism in this family, because there are no complications introduced by the presence of magnetic rare-earth elements.

YNi_2B_2C crystallizes in a body-centered tetragonal structure with a $ThCr_2Si_2$-type (space group $I4/mmm$, D_{4h}^{17}). The crystal structure is layer-like in the c axis, reminiscent of the high-T_c cuprate superconductors, consisting of two alternating layers of Ni_2B_2 and YC. Electronic structure studies show three dimensional (3D) character and so it is thought to be a conventional BCS type superconductor with a relatively high density of states (DOS) at the Fermi level [4–7]. Despite the layered anisotropic crystal structure, some physical properties of YNi_2B_2C are often considered to be isotropic. Note that the 3D character of the electronic structure does not necessarily mean the isotropy of physical properties. In fact, it has not yet been settled whether the physical properties of YNi_2B_2C are isotropic or not. Civale *et al.* [8] observed an anisotropic effective mass ratio $\gamma = (m_{max}/m_{min})^{1/2} \sim 1.1$, while Johnston-Halperin *et al.* [9] observed an isotropic result, $\gamma \sim 1.005$. Fisher *et al.* [10] reported isotropic resistivity for non-magnetic YNi_2B_2C and anisotropic resistivity for magnetic borocarbide superconductors like $ErNi_2B_2C$ and $HoNi_2B_2C$. Rathnayaka *et al.* [11] observed an isotropic upper critical field, H_{c2}, for YNi_2B_2C, but a small anisotropic H_{c2} for $LaNi_2B_2C$. In contrast, anisotropic properties were reported for YNi_2B_2C thin-films in the upper critical field [12], thermal conductivity [13], critical field for vortex lattice transition [14], and paramagnetic susceptibility from nuclear magnetic resonance (NMR) experiments [15]. von Lips *et al.* [16] used X-ray absorption spectroscopy (XAS) and the linear combination of atomic-like orbitals (LCAO) band method for YNi_2B_2C to determine the anisotropic nature of the unoccupied DOS.

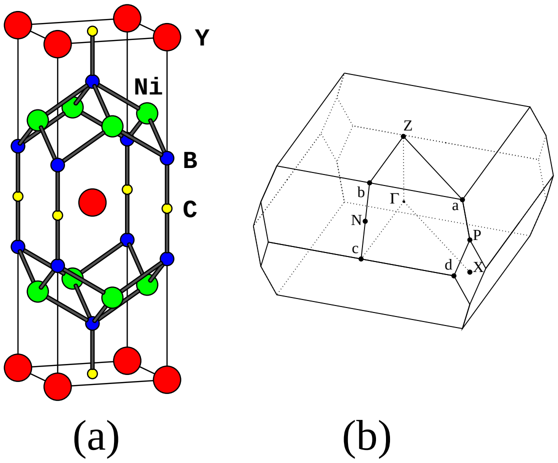

FIG. 1. (a) Crystal structure and (b) the first Brillouin zone of YNi_2B_2C.

The optical properties of YNi_2B_2C have been studied several times since the first measurement by Widder *et al.* [17], who obtained anisotropic results by linking together optical reflectance and electron energy loss spectroscopy (EELS) measurements. On the other hand, Bommeli *et al.* [18] reported that the structural anisotropy would not affect the optical data based on the observation that both the polycrystalline and single crystal samples produced equivalent experimental results. Therefore, the results were conflicting, and until recently, the anisotropy problem in the optical properties of Ni borocarbides has not been resolved [19–21]. It is important to understand correct optical properties since the superconducting energy gap is obtained from optical measurements [18].

Interestingly, all the above optical groups utilize the 3D electronic structures of Ni borocarbides for their experiments. It thus indicates that the electronic structure information only may not be enough to determine definitely the optical anisotropy. In this Letter, to resolve this controversial issue, the optical conductivity and the electron energy loss spectroscopy (EELS) have been studied theoretically for the first time by using first principles calculations. We have found that the optical properties of YNi_2B_2C are really anisotropic.

Calculations are performed by employing the highly precise first principles local density full-potential linearized augmented plane wave (FLAPW) method [22], which makes no shape approximations to the charge density or the potential. The Hedin-Lundqvist form [23] is employed for the LDA exchange-correlation energy. We used lattice parameters determined by experiment [24], 240 special **k**-points [25] for the self-consistency cycle and 8619 **k**-points for the calculation of the optical properties inside the irreducible Brillouin zone. The optical conductivity arises from the optical transitions of the occupied valence electrons to unoccupied states above E_F [26]. Each interband transition is broadened in the calculation by introducing a finite phenomenological inverse life time, Δ=0.05 eV. The Drude term due to free carriers is taken into account by using parameters from experiment [17].

Figure 1 shows the crystal structure and the first Brillouin zone of YNi_2B_2C. In Fig. 1(b), points a,b,c, and d are not symmetry points since the symmetry is not a local maximum at those points. Points a and d (and b and c likewise) are the same points by the translational symmetry in **k**-space. X has the highest symmetry as Γ with 16 symmetry elements.

Figure 2 shows the calculated energy band structures along the symmetry lines. Band dispersions agree well with existing calculations. However, in the present full-potential band calculation, the 19th band at Γ, which gives a small calabash shaped Fermi surface in the LMTO-ASA calculation [6], is lifted up to higher energy.

Figure 3 compares the calculated optical conductivities for YNi_2B_2C with experiments, in which σ_x and σ_z represent theoretical conductivities along the x and z directions, respectively. One can see a clear difference between σ_x and σ_z, implying the anisotropic nature of the optical conductivity. Anisotropic optical conductivities in the calculation are consistent with the anisotropy observed in the experiment by Widder *et al.* [17], represented by σ_x_w and σ_z_w in Fig. 3. Peaks are located at 2.48, 7.6, 8.9, and 9.6 eV for σ_x, and at 2.4, 5.0, 8.16, and 9.5 eV for σ_z in the calculation. The most prominent and anisotropic peak in the calculation is the one at 2.4 eV of σ_z, while σ_x has a peak at 2.48 eV with a smaller magnitude than σ_z. However, the intensity and position of the peak of σ_z are somewhat different from those in experiment: the highest peak is located at 1.6 eV, which is lower by 0.8 eV than the theoretical one. It is unusual that the experimental peak is located at lower frequency considering that, in most LDA calculations, theoretical peaks are found at lower frequencies than experimental ones. The disagreement is to be clarified further theoretically or experimentally. Other optical properties such as the reflectivity R and the dielectric constants ϵ show similar anisotropies which will be discussed elsewhere.

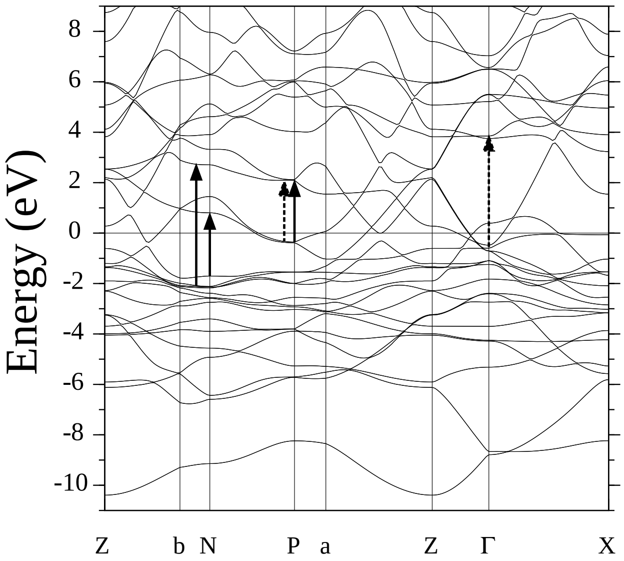

FIG. 2. Electronic energy band structure of YNi_2B_2C. Dot and solid arrows indicate typical interband transitions along the x and z directions, respectively (see text and Fig. 4).

Bommeli *et al.* [18] obtained isotropic optical conductivity (denoted by σ_x_b in Fig. 3). The overall shape of σ_x_b is seemingly close to σ_x_w, except that some fluctuations occur when the relative magnitude of σ_z_w with respect to σ_x_w becomes large. This feature can be understood if σ_x_b corresponds to the average of the anisotropic optical conductivity. Although it is not clear in σ_x_b, there is a peak at around the 2.4 eV in σ_x_w. The 2.4 eV peak in σ_x is also observed in a recent experiment by Lee *et al.* [20]. Hence the experimental peak at 2.4 eV can be assigned to the calculated σ_x peak at 2.48 eV,

The optical conductivity is obtained directly from the optical transitions between energy levels in the solid. Hence the peaks in the optical conductivity can be assigned to specific interband transitions. However, peaks in derived quantities from the optical conductivity, such as the reflectivity R and the refractive index n, may be shifted from the peaks of the optical conductivity. In order to identify the peaks manifested in the optical conductivity, we plot in Fig. 4 the momentum resolved optical conductivity $\sigma(\mathbf{k},\omega)$ along the symmetry lines in the Brillouin zone. Integrating $\sigma(\mathbf{k},\omega)$ over $\mathbf{k}$-space gives rise to the optical conductivity $\sigma(\omega)$.

Figures 4 (a) and (b) provide the optical transitions along the x and z directions, respectively. The darker intensity in Fig. 4 represents the stronger interband transitions. It is evident from Figs. 4(a) and (b) that the optical transitions are anisotropic between the x and z directions. The anisotropy is due to different matrix element between the x and z directions. Strong transitions in the z-direction occur around P and N, while they occur at points near Γ in the x-direction. The anisotropy is most prominent at the 2.4 eV transition near P; there is a strong transition in the z-direction, but a negligible transition in the x-direction. The intensity of the 2.4 eV transition is further enhanced by the transition near N. In Fig. 2, corresponding transitions for 2.4 eV are marked as small solid arrows at N and P. Other strong transitions identified in Fig. 4 are also marked as arrows in Fig. 2. It is noteworthy that the unoccupied bands (19th band) for the 2.4 eV transition near P have similar shapes to the occupied bands (18th band), reminiscent of the nesting of bands.

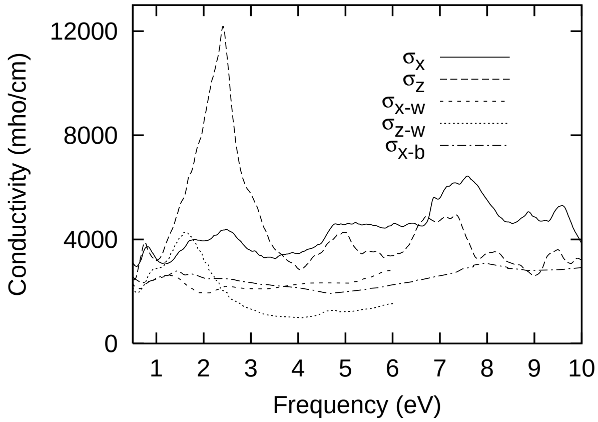

FIG. 3. Optical conductivity of YNi_2B_2C. σ_x and σ_z represent results from the calculation. Experimental data are taken from Ref. [17](σ_x-w and σ_z-w) and Ref. [18](σ_x-b).

In order to see the detailed nature of the transition, we have calculated contributions from each atomic species for the bands related to the 2.4 eV transition at P. The 18th band consists of Ni-$d_{3z^2-r^2}$(36%) and Ni-d_{xy}(35%) states, while the unoccupied band (19th band) consists of Ni-d_{xy}(16%), Ni-s(12%), Ni-p_z(4.4%), B-p(6.9%), and C-p(16%) states. Since the occupied band originates mainly from Ni-d states, the transition matrix element is determined by Ni site. By the selection rule about the symmetry of the wave functions, one can assign the 2.4 eV peak in σ_z to the transition between Ni-$d_{3z^2-r^2}$ and Ni-p_z. The transition matrix element for σ_x is zero in this case, which explains the negligible intensity at 2.4 eV near P in $\sigma_x(\mathbf{k},\omega)$. Thus Ni states play a vital role in yielding a large anisotropic peak in σ_z. This is indeed consistent with the dominant Ni-d DOS near the Fermi level [6].

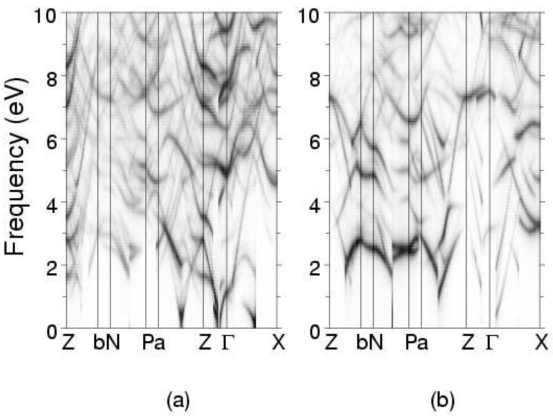

FIG. 4. Momentum resolved optical conductivity $\sigma(\mathbf{k},\omega)$ for (a) x and (b) z direction, respectively.

Figure 5 depicts the loss function, $\mathrm{Im}(-1/\epsilon(\omega))$, of the EELS measurement with zero momentum transfer. There is no EELS data available for single crystals. Hence, in the figure, the calculated result is compared with Widder *et al.*'s experiment for polycrystals [17]. There is no plasma peak due to free carriers which is expected to occur between 3.75 eV and 4.25 eV [17,19,20]. It is damped due to interband transitions (Landau damping), in agreement with the experimental EELS result. The calculated loss function shows a two peak structure in both the x and z-direction, and the spectrum in the z-direction is narrower and higher than that of x direction. Two peaks are located at 22.7 eV and 26 eV in the z-direction. In YNi_2B_2C, there are 33 valence electrons per formula unit. The simple plasma frequency relation, $\omega_p^2 = 4\pi ne^2/m$, gives 26.3 eV which agrees well with the above plasma frequency of 26 eV. Therefore, one can explain the plasma frequency at 26 eV as originating from the response of all valence electrons to the external electric field. Then the peak at 22.7 eV can be ascribed to the valence electrons near E_F: Ni-d, Y-d, B-p, and C-p states. In the experiment, two peaks are observed at $\sim$ 20 eV and $\sim$ 35 eV. Although the two peak structure in the calculation agrees qualitatively with experiment, the peak positions are different. The EELS experiment with single crystal is required to clarify the discrepancy between theory and experiment.

In conclusion, we have investigated the optical properties of YNi_2B_2C by using the first-principles FLAPW method. The optical conductivity is found to be anisotropic between the x and the z direction. A strong peak at 2.4 eV is obtained in the z direction, which is assigned to the transition near P between Ni-$d_{3z^2-r^2}$ and Ni-p_z states, indicating that the Ni-site plays an important role in the anisotropy of YNi_2B_2C. The calculated EELS spectra are also found to be anisotropic with a two peak structure.

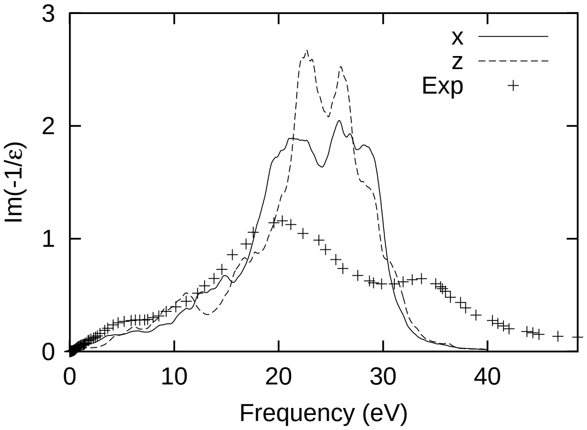

FIG. 5. Electron energy loss (EELS) spectrum $\mathrm{Im}(-1/\epsilon)$ of YNi_2B_2C. Crosses represent experimental data reproduced from the experimental Widder *et al.* [17].

ACKNOWLEDGMENTS

The authors are grateful to KISTEP/CRI of Korean ministry of Science and Technology for financial support. BIM is also supported by the KOSEF through the eSSC at POSTECH. SJY thanks to Prof. J. H. Kim for helpful discussions. Work at Northwestern University supported by the U.S. Department of Energy (Grant No. DE-F602-88ER45372).

---

[1] R. Nagarajan *et al.*, Phys. Rev. Lett. **72**, 274 (1994).
[2] R. J. Cava *et al.*, Nature **367**, 252 (1994).
[3] P. C. Canfield, P. L. Gammel, and D. J. Bishop, Phys. Today **51** (10), 40 (1998).
[4] L. F. Mattheiss, Phys. Rev. B **49**, 13 279 (1994).
[5] W. E. Pickett and D. J. Singh, Phys. Rev. Lett. **72**, 3702 (1994).
[6] J. I. Lee *et al.*, Phys. Rev. B **50**, 4030 (1994).
[7] D. J. Singh, Solid State Comm. **98**, 899 (1996).
[8] L. Civale *et al.*, Phys. Rev. Lett. **83**, 3920 (1999).
[9] E. Johnston-Halperin *et al.*, Phys. Rev. B **51**, 12852 (1995).
[10] I. R. Fisher, J. R. Cooper, and P. C. Canfield, Phys. Rev. B **56**, 10 820 (1997).
[11] K. D. D. Rathnayaka *et al.*, Phys. Rev. B **55**, 8506 (1997).
[12] R. Vaglio *et al.*, Phys. Rev. B **56**, 934 (1997).
[13] M. Sera *et al.*, Phys. Rev. B **54**, 3062 (1996).
[14] H. Sakata *et al.*, Phys. Rev. Lett. **84**, 1583 (2000).
[15] K. Kumagai *et al.*, J. Low Temp. Phys. **105**, 1641 (1996).
[16] H. von Lips *et al.*, Phys. Rev. B **60**, 11 444 (1999).
[17] K. Widder *et al.*, Europhys. Lett **30**, 55 (1995); K. Widder *et al.*, J. Low Temp. Phys. **105**, 516 (1996).
[18] F. Bommeli *et al.*, Phys. Rev. Lett. **78**, 547 (1997).
[19] J. H. Kim *et al.*, Physica C **341**, 2233 (2000).
[20] S. J. Lee, B. K. Cho, P. C. Canfield, and D. W. Lynch, Phys. Rev. B **63**, 233103 (2001).
[21] M.-O. Mun *et al.*, J. Kor. Phys. Soc. **39**, 406 (2001).
[22] E. Wimmer, H. Krakauer, M. Weinert, and A. J. Freeman, Phys. Rev. B **24**, 864(1981); M. Weinert, E. Wimmer, and A. J. Freeman, *ibid.* **26**, 4571(1982).
[23] L. Hedin and B. I. Lundqvist, J. Phys. C. **4**, 2064 (1971).
[24] N. M. Hong *et al.*, Physica C **227**, 85 (1994).
[25] H. J. Monkhorst and J. D. Pack, Phys. Rev. B **13**, 5188 (1976).
[26] M. Kim, A. J. Freeman, and R. Wu, Phys. Rev. B **59**, 9432 (1999).